Journal of Power Sources 196 (2011) 8904–8908

Contents lists available at ScienceDirect

Journal of Power Sources

journal homepage: www.elsevier.com/locate/jpowsour

Short communication

Enhanced efficiency of dye-sensitized solar cells through $TiCl_4$-treated, nanoporous-layer-covered TiO_2 nanotube arrays

Jeong-Hyun Park[a], Jae-Yup Kim[b], Jae-Hong Kim[a], Chel-Jong Choi[c], Hyunsoo Kim[c], Yung-Eun Sung[b,**], Kwang-Soon Ahn[a,*]

[a] School of Chemical Engineering, Yeungnam University, Gyeongsan 712-749, South Korea
[b] School of Chemical and Biological Engineering, Seoul National University, Seoul, South Korea
[c] School of Semiconductor and Chemical Engineering, Chonbuk National University, Jeonju, South Korea

ARTICLE INFO

Article history:
Received 26 April 2011
Received in revised form 17 June 2011
Accepted 20 June 2011
Available online 24 June 2011

Keywords:
Dye-sensitized solar cell
Nanotubes
Surface treatment
Electron lifetime
Electron transport

ABSTRACT

$TiCl_4$-treated, nanoporous-layer-covered TiO_2 (Type II) nanotube arrays are fabricated through a two-step anodization process followed by treatment with $TiCl_4$. A dye-sensitized solar cell (DSSC) with $TiCl_4$-treated, nanoporous-layer-covered Type II TiO_2 nanotubes is compared with other DSSCs based on untreated Type II and both untreated and $TiCl_4$-treated, conventional TiO_2 (Type I) nanotube arrays. The $TiCl_4$ surface treatment's effects on dye adsorption, charge transport, and electron lifetime are dependent on the morphologies of the TiO_2 nanotubes. The $TiCl_4$-treated Type I nanotubes allow higher dye adsorption, whilst the $TiCl_4$-treated Type II nanotubes provide much faster electron transport and enhanced electron lifetime. This is because there are fewer defect traps in the nanostructure well-aligned without bundling, which contributes to the significantly improved cell performance over the DSSC with the $TiCl_4$-treated Type I nanotubes.

1. Introduction

TiO_2-based dye-sensitized solar cells (DSSCs) have attracted much attention because of their potential to be low-cost alternatives to commercial Si-based solar cells [1–3]. DSSCs consist of a dye-sensitized TiO_2 layer and a Pt counter electrode, with an electrolyte containing a redox couple (I^-/I_3^-) between them.

Cell performance has been improved mainly by controlling the surface morphology and/or particle size of the TiO_2 layer [4,5], and by developing new dyes [6], and electrolytes [7]. Conventional mesoporous TiO_2 films composed of nanoparticles smaller than 30 nm do not develop a depletion layer at the interface between the TiO_2 and electrolyte. This causes large back electron transfer from the conduction band of the TiO_2 to the electrolyte due to trap-limited diffusion [8,9]. Suppression of back electron transfer has been attempted by employing 1-dimensional nanostructures (nanotubes, nanorods, *etc.*) with faster electron transport and slower recombination rates [5,10–12]. However, nanostructured DSSCs based on nanotube arrays have not exhibited efficiencies as high as those obtained with nanoparticles, mainly because of reduced dye adsorption by their lower surface areas [13,14].

Post-treatment of mesoporous TiO_2 films with $TiCl_4$ solution has been used to increase cells' efficiencies. $TiCl_4$ surface treatment has been reported to increase surface area and improve electron transport, light scattering, purification of TiO_2 and anchoring of dyes [4,12,13,15–18]. Although the treatment's effect strongly depends on the starting TiO_2 material to which it is applied, it has scarcely been studied [18].

In this paper, two types of TiO_2 nanotubes were synthesized as different starting materials for $TiCl_4$ surface treatment: conventional TiO_2 nanotube arrays (Type I) and nanoporous-layer-covered TiO_2 nanotube arrays (Type II). The $TiCl_4$ surface treatment's effects on the morphologies of the TiO_2 nanotubes were studied in terms of dye adsorption, charge transport, and electron lifetime. We found that $TiCl_4$ treatment of the Type II nanotubes, which had fewer defects, led to relatively faster electron transport and enhanced electron lifetime. As a result, a DSSC containing $TiCl_4$-treated Type II nanotubes exhibited enhanced overall energy conversion efficiency compared with a DSSC containing $TiCl_4$-treated, conventional Type I nanotubes.

2. Experimental

2.1. Conventional TiO_2 nanotubes (1-step nanotubes, Type I) grown on the Ti foils

Ti foil (Goodfellow, 0.1 mm thickness, 99.6% purity) was used for the anodic growth of TiO_2 nanotubes. It was roughly ground,

* Corresponding author. Tel.: +82 53 810 2524; fax: +82 53 810 4631.
** Corresponding author.
E-mail addresses: ysung@snu.ac.kr (Y.-E. Sung), kstheory@ynu.ac.kr (K.-S. Ahn).

0378-7753/$ – see front matter © 2011 Elsevier B.V. All rights reserved.
doi:10.1016/j.jpowsour.2011.06.063

cleaned by sonication in acetone and ethanol and then rinsed in de-ionized water (DI). Electrochemical anodization was conducted at 60 V for 4 h with *ca.* 4 cm separation between the working (Ti foil) and the counter electrode (Pt mesh) in all cases. The electrolyte consisted of 0.25 wt.% NH_4F in ethylene glycol containing a 1 M water. The 21 μm-thick, anodic TiO_2 nanotubes were sonicated in ethanol for 5 min to remove remnants from the surfaces and then dried in an air stream. They were then annealed at 450 °C for 4 h in air for improved crystallinity.

2.2. Nanoporous-layer-covered TiO_2 nanotubes (2-step nanotubes, Type II) grown on the Ti foils

Pretreated Ti substrates were first prepared by the 1-step electrochemical formation of conventional TiO_2 nanotubes. These were then peeled off from the Ti substrate by sonication in DI water for 5 min. A second anodization to form the 21 μm-thick, nanoporous-layer-covered TiO_2 nanotube arrays was performed under similar conditions to those of the 1-step TiO_2 nanotubes. The resulting 2-step TiO_2 nanotubes were sonicated in ethanol for 5 min to remove remnants from their surfaces and then dried in an air stream. They were annealed at 450 °C for 4 h in air to convert the amorphous phase to an anatase structure.

2.3. $TiCl_4$ post-treatment

Post-treatment with $TiCl_4$ has been applied by being soaked in a 40 mM $TiCl_4$ aqueous solution for 30 min at 70 °C. After flushing with ethanol and drying, the electrodes were sintered again at 450 °C for 30 min.

2.4. Cell fabrication

Samples were dye-sensitized with Ru-based N3 dye [cis-bis (4,4′-dicarboxy-2,2′-bipyridine) dithiocyanato ruthenium (II)] (Solaronix SA, Switzerland) by being immersed in dye solution at 40 °C for 24 h. Semitransparent Pt counter electrodes were prepared by doctor-blading the Pt nanocluster-containing Pt paste (PT-1, Dyesol. Ltd.) on the F-doped SnO_2 (FTO) transparent conducting substrates followed by the calcination at 450 °C for 30 min in air. The dye-adsorbed TiO_2 nanotube photoanodes and semitransparent Pt counter electrodes were sandwiched with a liquid electrolyte containing the redox couple (I^-/I_3^-) introduced between them. All samples had similar active areas of dye-adsorbed photoanodes, 0.24 cm^2.

2.5. Characterization

The DSSCs were illuminated from the back-side, *i.e.*, from the semitransparent Pt counter electrode side (back-illumination) and those photovoltaic current-voltage characteristics were measured under 1 Sun illumination (100 mW cm^{-2}, AM 1.5) verified by an AIST-calibrated Si-solar cell. Nyquist plots were measured between 1 Hz and 100 kHz using an electrochemical impedance analyzer under 1 Sun at open-circuit potential.

For open-circuit voltage decay (OCVD) measurement, cells were illuminated to a steady voltage. The illumination was then cut off by a shutter. The decay analyses refer only to values measured after the shutter obtained full darkness. Incident photon-to-current conversion efficiency (IPCE) was measured on an action spectrum measurement setup (PEC-S20, Peccell Ltd.). UV–vis spectra were taken of dye molecules desorbed from the TiO_2 in 1 M aqueous NaOH. The TiO_2 nanotube arrays' morphologies were characterized by scanning electron microscopy (SEM, Hitachi FE-SEM S4800).

3. Results and discussion

Fig. 1(a) and (c) shows SEM images viewed from the top of the Type I TiO_2 nanotube arrays. The Type I sample comprised separated nanotubes with average diameter and wall thickness of 90 (±7) nm and 11 nm, respectively. The 21 μm-thick, nanoporous-layer-covered TiO_2 nanotubes (Type II) were prepared by removing the Type I nanotubes followed by the second anodization. Fig. 1(b) and (d) shows the SEM images viewed from the top of the Type II nanotube arrays. Fig. 1(d) and its inset show that each nanopore corresponds to one nanotube (average diameter, 100 (±10) nm; average wall thickness, 11 nm) and the void areas on the surface are covered with a thin nanoporous TiO_2 layer [19]. The Type I sample exhibited the bundling of the nanotubes, due to liquid-meniscus-induced capillary forces, which causes many defects

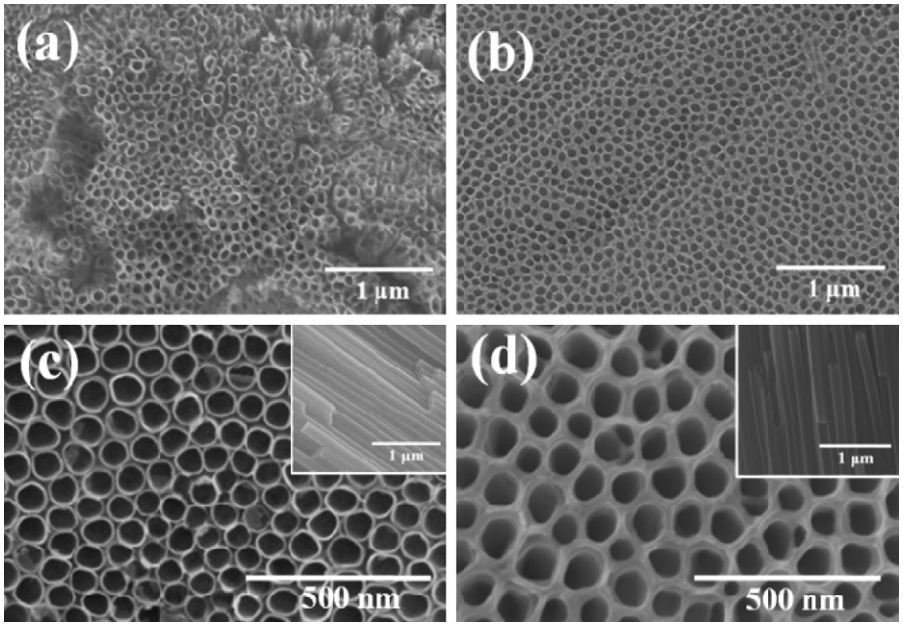

Fig. 1. FE-SEM surface morphologies of (a and c) the conventional TiO_2 nanotube arrays (Type I) and (b and d) nanoporous-layer-covered TiO_2 nanotube arrays (Type II). Insets are cross-sectional images.

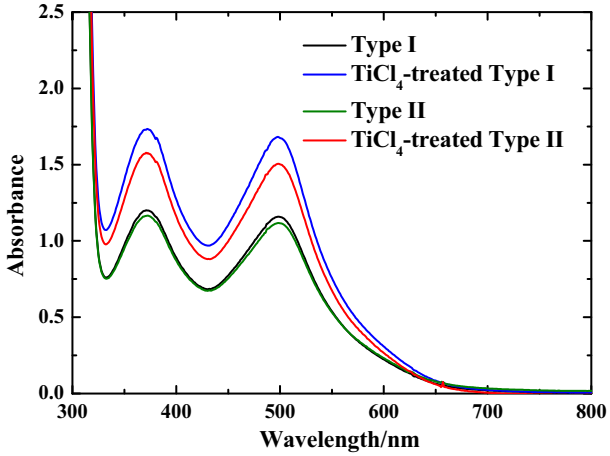

Fig. 2. UV–vis absorbance spectra of the dye molecules detached from the nanotubes with and without the $TiCl_4$ treatment by 0.1 M NaOH aqueous solution.

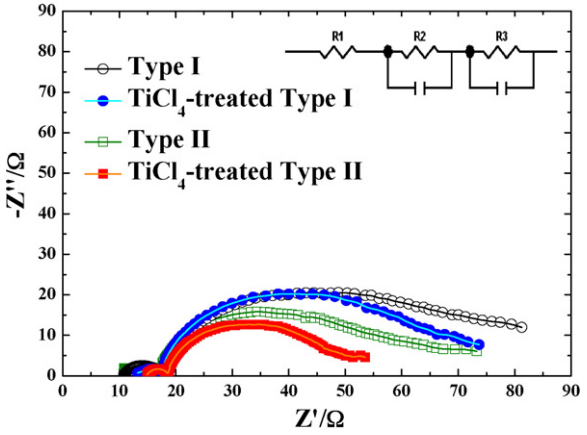

Fig. 3. Nyquist plots of DSSCs based on TiO_2 nanotube arrays (Types I and II) with and without $TiCl_4$ post-treatment measured at V_{oc} under 1 Sun illumination.

(recombination centers) [19]. In contrast, the Type II nanotubes have relatively fewer defects, because the surface-interconnected nanopores help to keep the nanotubes in a parallel arrangement and prevent them from bundling, as shown in Fig. 1(b) [19]. This difference in morphology may have a significant influence on the effects of the $TiCl_4$ surface treatment.

There was no apparent morphological difference for the nanotubes (Types I and II) before and after the $TiCl_4$ post-treatments, due to the use of low concentration (40 mM) of the $TiCl_4$ solution. Fig. 2 shows the UV–vis absorbance spectra of the dye molecules detached from the nanotubes with and without the $TiCl_4$ treatment by 0.1 M NaOH aqueous solution. The amounts of adsorbed N3 dye, measured using UV–vis spectroscopy, were 3.51×10^{-7}, 5.08×10^{-7}, 3.38×10^{-7}, and 4.55×10^{-7} mol cm^{-2} for Type I, $TiCl_4$-treated Type I, Type II, and $TiCl_4$-treated Type II samples, respectively. The extent of dye adsorption on the TiO_2 corresponds to its active surface area which facilitates the anchoring of the dyes [13,15]. The Type I sample exhibited greater adsorption than the Type II, indicating a higher active surface area. $TiCl_4$ surface treatment increased the amount of adsorbed dye for both Types I and II. It may be due to the purification and passivation of the TiO_2 surface, leading to the increased active surface area [4,12,13,15–18]. The $TiCl_4$-treated Type II nanotubes exhibited less adsorbed dye than the treated Type I nanotubes, because of lower surface area.

Fig. 3 shows Nyquist plots of DSSCs made from both types of nanotubes with and without the $TiCl_4$ treatment. Measurements were taken at open circuit voltage (V_{oc}) under 1 Sun illumination. The semicircles at high- and low-frequencies arose from electrochemical reaction resistance at the Pt counter electrode (R2, inset Fig. 3) and charge transfer resistance at the TiO_2/dye/electrolyte interface (R3, inset Fig. 3) [15,20]. The Type II cells exhibited lower R3 than the Type I, indicating faster electron transport due to fewer traps (or recombination centers) in the well-aligned arrays. $TiCl_4$ surface treatment reduced R3 in cells with both types of nanotube through surface passivation of trap states [13,15,20]. The $TiCl_4$-treated Type II cell had a much lower R3 than the $TiCl_4$-treated Type I cell, indicating much faster electron transport. Therefore, the $TiCl_4$ surface treatment of a less defective morphology led to significantly improved electron transport.

Electron lifetimes were estimated through open circuit voltage decay (OCVD) measurements [4,21]. Fig. 4(a) shows V_{oc} decay curves of DSSCs with both types of nanotube with and without $TiCl_4$ treatment recorded during relaxation from an illuminated quasi-equilibrium state to the dark equilibrium. Fig. 4(b) shows electron lifetimes calculated from the OCVD curves, according to [4,21]:

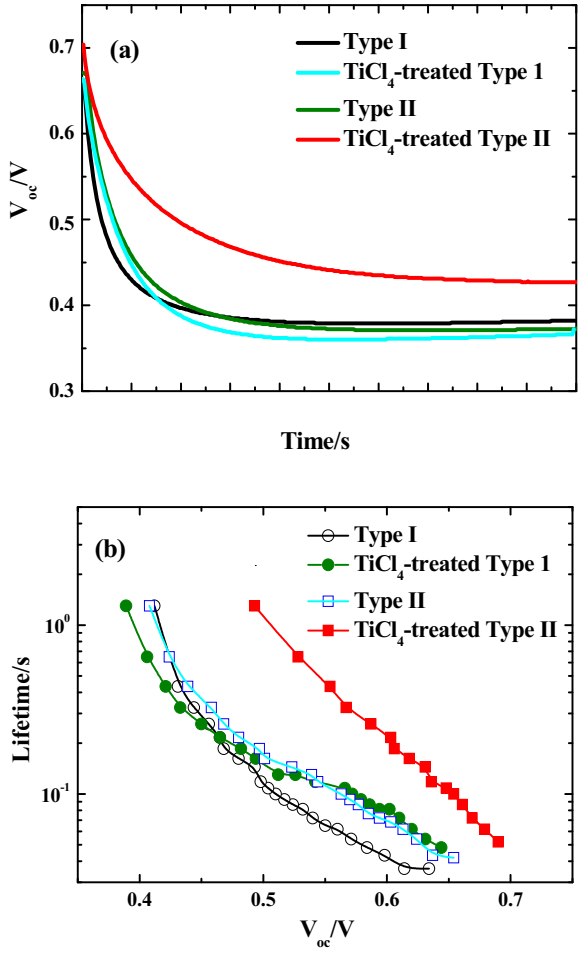

Fig. 4. (a) V_{oc} decay curves of DSSCs based on TiO_2 nanotube arrays (Types I and II) with and without the $TiCl_4$ post-treatment recorded during relaxation from an illuminated quasi-equilibrium to the dark equilibrium. (b) Electron lifetimes estimated from (a).

$$\tau_e = -\frac{k_B T}{e}\left[\frac{dV_{oc}}{dt}\right]^{-1} \quad (1)$$

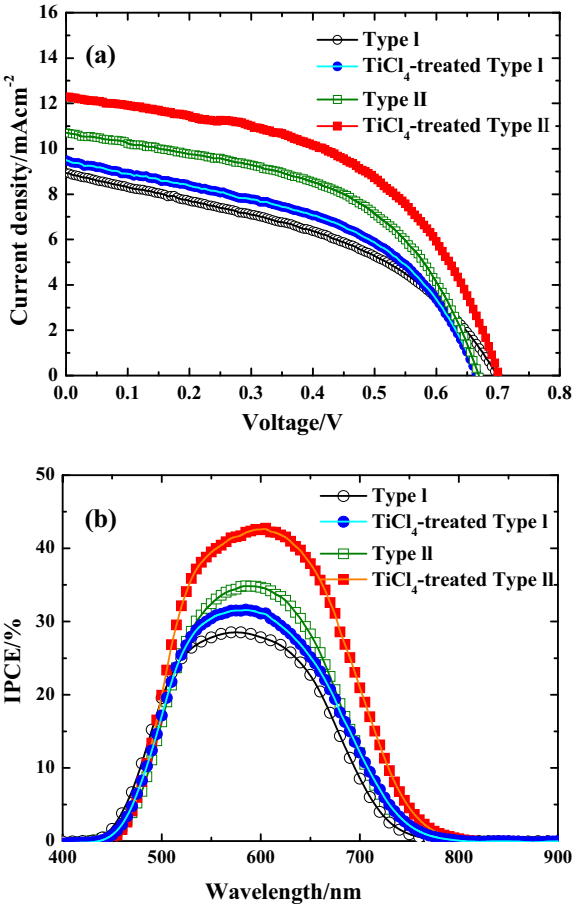

Fig. 5. (a) Photocurrent-voltage curves of DSSCs based on the TiO_2 nanotube arrays (Types I and II) with and without the $TiCl_4$ post-treatment measured under 1 Sun illumination. (b) IPCE (incident photon-to-current efficiency) curves.

where the k_BT is the thermal energy, e is the positive elementary charge, and dV_{oc}/dt is the derivative of the open circuit voltage transient. The photovoltage decay rate is directly related to electron lifetime; because, as the illumination of the DSSC at open circuit is interrupted, excess electrons are removed through recombination. The Type II cell exhibited longer electron lifetime than the Type I (with conventional nanotube arrays) (Fig. 4(b)), indicating that the Type II had fewer recombination centers because of its well-aligned nanostructure having fewer surface defects. The $TiCl_4$-treated, nanoporous-layer-covered TiO_2 nanotube arrays exhibited significantly improved electron lifetime, compared with the $TiCl_4$-treated, conventional nanotubes. This can be attributed to not only much fewer defect sites in the nanostructure well-aligned without bundling but also to the passivation effect of the $TiCl_4$ treatment on the surface trap states.

$TiCl_4$ surface treatment was beneficial to the amount of the adsorbed dye, electron transport, and electron lifetime. Furthermore, the effect of the treatment depended on the morphology of the nanotubes. $TiCl_4$ treatment of the Type I (conventional) nanotubes led to more increased dye adsorption, compared with the $TiCl_4$-treatment of the Type II nanotubes. However, the $TiCl_4$-treated Type II nanotubes provided remarkably improved electron transport and electron lifetime. Fig. 5(a) shows photovoltaic performances of the four DSSCs measured under 1 Sun illumination (summarized in Table 1). $TiCl_4$ post-treatment enhanced overall energy conversion efficiencies in cells of both types, because of increased dye adsorption, improved charge transport, and reduced recombination. The effects of $TiCl_4$ surface treatment on dye

Table 1
Photovoltaic performances of DSSCs based on TiO2 nanotube arrays (Types I and II) with and without $TiCl_4$ post-treatment.

Samples	J_{sc} (mA cm^{-2})	V_{oc} (V)	FF (%)	η (%)	Dye (mol cm^{-2})
Type I	8.9	0.70	42.55	2.7	3.51×10^{-7}
$TiCl_4$-treated Type I	9.5	0.67	47.01	3.0	5.08×10^{-7}
Type II	10.7	0.67	50.45	3.6	3.38×10^{-7}
$TiCl_4$-treated Type II	12.3	0.70	50.90	4.4	4.55×10^{-7}

adsorption, charge transport, and electron lifetime were dependent on the nanostructural morphologies, as discussed above. The DSSC with $TiCl_4$-treated Type II nanotubes resulted in a cell efficiency (4.4%) improved by 22% over that of the cell using untreated Type II nanotubes. The efficiency (3.0%) of the DSSC with $TiCl_4$-treated Type I nanotubes was increased 11% over that of the DSSC with untreated Type I nanotubes. The efficiency gains by $TiCl_4$ treatment were mainly dominated by increased short-circuit current (J_{sc}); this was studied in more detail using the incident photon-to-current efficiency (IPCE) curves (Fig. 5(b)). IPCE is influenced by three factors, according to [18]:

$$\mathrm{IPCE} = \mathrm{LHE} \cdot \eta_{\mathrm{inj}} \cdot \eta_{\mathrm{cc}} \quad (2)$$

where LHE is the light-harvesting efficiency, η_{inj} is the charge-injection efficiency, and η_{cc} is the charge-collection efficiency. η_{inj} was close to unity, due to the fast electron injection from the excited N3 dye to the TiO_2. LHE was determined by the amount of adsorbed dye, light scattering, and the concentration of redox species [18]. In Fig. 2, the amount of the adsorbed dyes of the $TiCl_4$-treated Type I was higher than that of the $TiCl_4$-treated Type II, indicating that the $TiCl_4$-treated Type I provides higher LHE value. However, the $TiCl_4$-treated Type II cell exhibited much higher IPCE than the $TiCl_4$-treated Type I cell, despite having less adsorbed dye. Instead, the improved cell efficiency of the DSSC with the $TiCl_4$-treated Type II nanotubes may be related to the charge-collection efficiency (η_{cc}). η_{cc} is largely determined by the competition between recombination and charge transport. Figs. 3 and 4 show that the $TiCl_4$-treated Type II sample exhibited faster electron transport and improved electron lifetime, compared with the $TiCl_4$-treated Type I sample, because of fewer trap sites in the nanostructure well-aligned without bundling. Therefore, although the $TiCl_4$-treated Type II cell exhibited less adsorbed dye compared with the $TiCl_4$-treated Type I cell, it had a significantly improved IPCE and overall energy-conversion efficiency because of the enhanced η_{cc}. That is, significantly improved cell performance of the DSSC with the $TiCl_4$-treated Type II nanotube can be attributed to remarkably enhanced electron lifetime and much faster charge transport in addition to the increase of the active surface area for the adsorption of the dyes.

4. Conclusions

In summary, a DSSC with $TiCl_4$-treated, nanoporous-layer-covered Type II TiO_2 nanotubes was fabricated and compared with other DSSCs based on untreated Type II and both untreated and $TiCl_4$-treated Type I (conventional) nanotubes. The $TiCl_4$ surface treatment's effects on dye adsorption, charge transport, and electron lifetime were dependent on the morphologies of the TiO_2 nanotubes. The $TiCl_4$-treated Type I nanotubes allowed higher dye adsorption, whilst the $TiCl_4$-treated Type II nanotubes provided much faster electron transport and enhanced electron lifetime. This was because there were fewer defect traps in the nanostructure well-aligned without bundling, which contributed to the improved cell performance over the DSSC with the $TiCl_4$-treated Type I nanotubes. Although more detailed studies of the $TiCl_4$ treatment of nanostructured morphologies are needed, these findings should provide good insight into the surface treatment of nanostructured

films for diverse applications including DSSCs, photoelectrochemical water-splitting cells, and batteries.

Acknowledgements

This research was supported by the Basic Science Research Program through the National Research Foundation of Korea (NRF) funded by the Ministry of Education, Science and Technology (grant number 2010-0003968) and the Human Resources Development Program of Korea Institute of Energy Technology Evaluation and Planning (KETEP) grant (number 20104010100580) funded by the Korean Ministry of Knowledge Economy.

References

[1] B. O'Regan, M. Grätzel, Nature 353 (1991) 737.
[2] J.P. Lee, B. Yoo, T. Suresh, M.S. Kang, R. Vital, K.J. Kim, Electrochim. Acta 54 (2009) 4365.
[3] M. Grätzel, Nature 414 (2001) 338.
[4] G.K. Mor, K. Shankar, M. Paulose, O.K. Varghese, C.A. Grimes, Nano Lett. 6 (2006) 215.
[5] Y.C. Nah, I. Paramasivam, P. Schmuki, ChemPhysChem 11 (2010) 2698.
[6] J.H. Yum, I. Jung, C. Baik, J.J. Ko, M.K. Nazeeruddin, M. Grätzel, Energy Environ. Sci. 2 (2009) 100.
[7] M.S. Kang, K.S. Ahn, J.W. Lee, Y.S. Kang, J. Photochem. Photobiol. A: Chem. 195 (2008) 198.
[8] M.D. Archer, A.J. Nozik, et al., in: R.J.D. Miller, R. Memming (Eds.), Nanostructured and Photoelectrochemical Systems for Solar Photon Conversion, Imperial College Press, Singapore, 2008, p. 130 (Chapter 2).
[9] K.-S. Ahn, M.S. Kang, J.K. Lee, B.C. Shin, J.W. Lee, Appl. Phys. Lett. 89 (2006) 013103.
[10] J.M. Nacak, H. Tsuchiya, L. Taveira, S. Aldabergerova, P. Schmuki, Angew. Chem. Int. Ed. 44 (2005) 7463.
[11] S.H. Kang, Y.S. Kim, J.Y. Kim, Y.E. Sung, Nanotechnology 20 (2009) 355307.
[12] M. Paulose, K. Shankar, O.K. Varghese, G.K. Mor, C.A. Grimes, J. Phys. D: Appl. Phys. 39 (2006) 2498.
[13] P. Charoensirithavorn, Y. Ogomi, T. Sagawa, S. Hayase, S. Yoshikawa, J. Electrochem. Soc. 157 (2010) B354.
[14] C.T. Yip, C.S.K. Mak, A.B. Djurišić, Y.F. Hsu, W.K. Chan, Appl. Phys. A 92 (2008) 589.
[15] S.-Y. An, J.-H. Park, J.-H. Kim, C.-J. Choi, H.S. Kim, K.-S. Ahn, J. Nanosci. Nanotechnol., in press.
[16] P. Roy, D. Kim, I. Paramasivam, P. Schmuki, Electrochem. Commun. 11 (2009) 1001.
[17] N. Fuke, R. Katoh, A. Islam, M. Kasuya, A. Furube, A. Fukui, Y. Chiba, R. Komiya, R. Yamanaka, L. Han, H. Harima, Energy Environ. Sci. 2 (2009) 1205.
[18] B.C. O'Regan, J.R. Durrant, P.M. Sommeling, N.J. Bakker, J. Phys. Chem. C 111 (2007) 14001.
[19] D. Wang, B. Yu, C. Wang, F. Zhou, W. Liu, Adv. Mater. 21 (2009) 1964.
[20] S. Sun, L. Gao, Y. Liu, Appl. Phys. Lett. 96 (2010) 083113.
[21] A. Zaban, M. Greenshtein, J. Bisquert, ChemPhysChem 4 (2003) 859.